DOI: 10.1002/cctc.200((will be filled in by the editorial staff))

The Mechanism of By-side Reactions in Alkane C-H Bond Functionalization by Coinage Homoscorpionate Complexes: A DFT study

Ataualpa A. C. Braga,[a] Ana Caballero,[b] Juan Urbano,[b] M. Mar Diaz-Requejo,[b] Pedro J. Pérez*[b] and Feliu Maseras*[a],[c]

DFT computational methods have been applied to the study of the mechanism for the formation of fumarate and maleate derivatives in a solution containing alkane, $Tp^{Br3}M$ (M = Cu, Ag; Tp^{Br3} = hydrotris(3,4,5-tribromopyrazolyl)borate ligand) and methyl diazoacetate. These are the experimentally reported conditions for carbene insertion into alkane C-H bonds, a procedure that usually competes with a non-desired reaction producing fumarate/maleate derivatives. Several mechanisms have been analyzed, the preferred one proceeding through direct reaction between a metallocarbene complex intermediate and a diazo compound molecule. The computational results explain all available experimental evidences, and provide important information toward the design of more efficient catalysts.

Introduction

Raw hydrocarbons constitute one of the most interesting potential sources of inexpensive precursors for the chemical industry. However, the development of efficient strategies to selectively produce functionalized adducts remains a challenge.[1,2] One of the emerging strategies in this field consists of the formal insertion of carbene units into C-H bonds catalyzed by transition metal complexes (Scheme 1a), a methodology that has expanded in the last decade as an efficient method to functionalize alkane carbon bonds.[3,4] Unfortunately, a competing reaction in which the diazo compound dimerizes appear as the main drawback of this transformation (Scheme 1b).

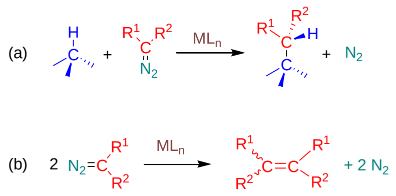

Scheme 1. (A) Functionalization of C-H bonds by carbene insertion. (b) The side-reaction leading to olefins.

[a] Dr. A. A. C. Braga, Prof. Dr. F. Maseras
Institute of Chemical Research of Catalonia (ICIQ), 43007 Tarragona, Catalonia, Spain
Fax: (+34) 977 920 231
E-mail: fmaseras@iciq.es

[b] Dr. A. Caballero, Dr. J. Urbano, Dr. M. Mar Dìaz-Requejo, Prof. Dr. P. J. Pérez
Laboratorio de Catálisis Homogénea, Departamento de Química y Ciencia de los Materiales, Unidad Asociada al CSIC, Universidad de Huelva, Campus de El Carmen, 21007 Huelva, Spain
E-mail: perez@dqcm.uhu.es

[c] Prof. Dr. F. Maseras
Departament de Química, Universitat Autônoma de Barcelona, 08193 Bellaterra, Catalonia, Spain

Supporting information for this article is available on the WWW under http://dx.doi.org/10.1002/cctc.200xxxxxx.((Please delete if not appropriate))

As part of that development, it has been reported that catalysts with general formula Tp^xML (M = Cu, Ag; Tp^x = trispyrazolylborate ligand, Figure 1; L = acetone, acetonitrile) can mediate the insertion of a carbene unit into a variety of alkane C-H bonds, being often used the ethyl diazoacetate (EDA) as carbene source.[5,6] Scheme 2 presents the generally accepted mechanism for the transition metal-mediated carbene transfer.

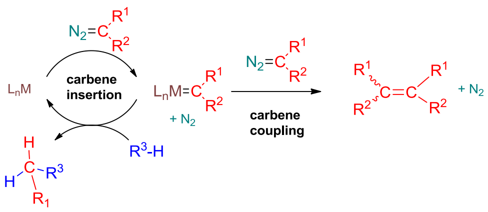

Scheme 2: Metal-catalyzed functionalization of C-H bonds and formation of fumarate/maleate derivatives by carbene transfer from diazo compounds.

The catalyst ML_n reacts with a diazo reagent to give the transient metallocarbene complex $L_nM{=}CR^1R^2$.[7] This type of intermediate is crucial to explain the presence of species with enough electrophilicity to insert carbene units into alkane C-H bonds. However, the increase in the reactivity also leads to undesired side-reactions.[3,4]

Detailed mechanistic insights into these processes have been obtained by computational studies,[8-10]. In a previous work[9] we have reported a detailed computational study on the mechanism involved in the metal-catalyzed carbene insertion into saturated C-H bonds of H_3C-H, $(CH_3)H_2C$-H, $(CH_3)_2HC$-H, and $(CH_3)_3C$-, as

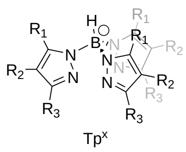

Figure 1. The hydrotrispyrazolylborate ligands.

representative examples of the simplest primary, secondary and tertiary saturated C-H bonds. The complexes $Tp^{Br3}M$ (Tp^{Br3} : $R^1 = R^2 = R^3$ = Br in Figure 1; M = Cu or Ag) and the carbene unit $:CHCO_2Me$ were studied, the calculations reproducing and explaining the experimental relative reactivity of C-H bonds and of the metal complexes.

Although such work clarified the mechanism of carbene insertion into C-H bonds of alkanes, the presence of competing side-reactions was not considered. The main side-reaction is the formation of diethyl maleate and diethyl fumarate, which can be formally viewed as the two possible isomers resulting from carbene dimerization (see Scheme 2). This side-reaction is a serious competition to carbene insertion, which can in some cases be totally suppressed. The mechanism for this side-reaction is so far unknown, and its investigation is the goal of the current work. There are some additional experimental data that must be also taken into account and explained by a mechanistic proposal. The first of them is that for the case of copper catalysts, the insertion reaction only proceeds when the diazo compound is added very slowly to the reaction media. If the diazo compound is added too fast, only the fumarate/maleate sideproducts are observed.[5] This constraint does not exist for the case of silver complexes.[6a] A second relevant experimental information is that in the case of silver complexes both insertion and fumarate/maleate formation are inhibited upon addition of a high excess of EDA. In this case, the reaction stops down, the reactants remaining as such. Finally, a previous work from our laboratories[11] showed that the use of very low concentrations of the copper catalysts causes a decrease in the formation of the non-desired products.

In this manuscript we have analyzed with the tools of computational chemistry the mechanism of the competing processes, in order to understand it and with the goel of the design of more efficient catalytic systems that can minimize the formation of byproducts.

Results and Discussion

Scheme 3 presents our proposal for the reactions that may take place in the reaction media. **PathA** is the generally accepted pathway for the carbene insertion into the C-H bond. **PathB**, **pathC** and **pathD** present three possible mechanisms for the competitive formation of fumarate and maleate sideproducts. Both fumarate and maleate come from the condensation of two

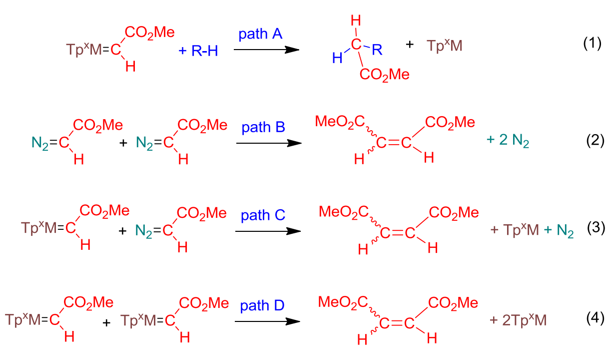

Scheme 3: Metal-catalyzed C-H functionalization through metallocarbene intermediate: carbene transfer from transient metallocarbene to C-H bond (eq. 1); carbene coupling between two diazo compounds (eq. 2); carbene coupling between metallocarbene species and diazo compounds (eq.3); metallocarbene coupling (eq 4).

carbene units, that can be formally provided either by the starting diazocompound or the metallocarbene intermediate. In **pathB**, there is a direct reaction between two diazocompounds whereas in **pathC** the reaction takes place between a diazo compound and a metallocarbene complex. Finally, in **pathD**, the production of maleate/fumarate derivatives results from the homocoupling of two metallocarbenes (**MC**) complexes.

We present below our computational results for the mechanisms in paths **A**, **B** and **C**. For the former, a summary of our previous report[9] is provided. For **pathD**, a transition state between two **MC** complexes has resulted elusive. We consider that this is due to the steric hindrance between the Tp^{Br3} ligands that makes the process impossible. In any case, this hypothetical pathway does not seem necessary to explain the experimental observations.

PathA

This is the mechanism for the functionalization of the C-H bonds by carbene insertion. In a previous work we reported a detailed computational study that also contained a full conformational analysis of the possible structures. Figure 2 shows the general pattern obtained and Table 1 displays the calculated energy values for the reaction between $Tp^{Br3}M{=}C(H)(CO_2CH_3)$ (M = Cu, Ag) and a variety of alkanes.

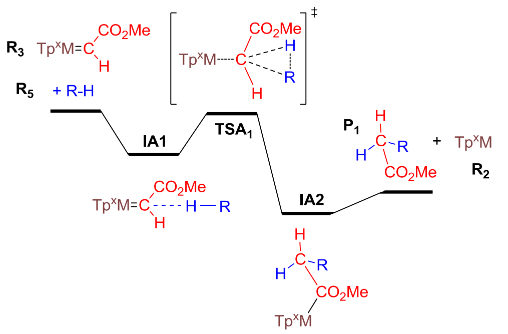

Figure 2: General pattern of the reaction between $Tp^{Br3}M{=}C(H)(CO_2CH_3)$ and R-H giving C(R)(H)2(CO2CH) and N_2

As shown in Figure 2, the alkanes R-H approach **MC** and form **IA1**, a van der Waals complex. This is followed by the carbene insertion into an alkane C-H bond through transition

Table 1. Potential energy (in kcal/mol) for the reaction between $Tp^{Br3}M{=}C(H)(CO_2CH_3)$ (M=Ag,Cu) and alkanes R-H to give $C(R)(H)_2(CO_2CH_3)$ and N_2.

M	R	IA1	TSA1	IA2	R1 + P1
Ag	CH_4	-0.7	3.8	-72.2	-61.2
	CH_3CH_3	-0.7	-0.1	-72.7	-62.4
	$(CH_3)_2CH_2$	-1.05	-1.04	-73.4	-63.4
	$(CH_3)_3CH$	—	—	-71.9	-61.9
Cu	CH_4	-0.6	10.0	-61.4	-49.8
	CH_3CH_3	-0.6[a]	5.4	-61.5	-51.1
	$(CH_3)_2CH_2$	-0.7	4.0	-70.3	-52.1
	$(CH_3)_3CH$	-0.6	4.0	-68.0	-50.6

[a] In this case the lower pathway takes place through the oxy face.

state **TSA1**. This process is concerted and leads to intermediate **IA2**, where the insertion has already taken place. By examination of the results collected in Table 1 we concluded that: (i) the activation barrier for the functionalization of C-H bonds catalyzed by **MC** complexes decreases in the order methane C-H > primary C-H > secondary C-H > tertiary C-H, and (ii) silver catalysts are more reactive than the corresponding copper complexes. The highest energy point in the pathway is transition state **TSA1**, therefore this one will be the reference to be compared with those of competing pathways.

PathB

In **PathB**, the coupling of two diazo compounds results in the fumarate/maleate derivatives. The pathways leading to each of the two isomeric side products are very similar. For clarity, we have labelled the structures with **ma** or **fu** suffixes. Figure 3 shows the energy profiles for the reaction. The first intermediates **IB1ma** and **IB1fu** are van der Waals species formed by two N_2=C(H)(CO_2CH_3) compounds. Their energies referred to the separated reactants have been calculated as -4.3 kcal/mol and -6.4 kcal/mol, respectively. The next step corresponds to the formation of the carbon-carbon bond between the carbene fragments, that occurs simultaneously to the departure of the two nitrogen molecules. The transition states to the formation of maleate (**TSB1ma**) and fumarate (**TSB1fu**) derivatives display high potential energy barriers of 40.0 and 40.7 kcal/mol, respectively. These values around 40 kcal/mol are prohibitive, and cannot compete with the very low barriers in **pathA** reported above. In fact, this **pathB** has been introduced in the analysis for the sake of completeness, but it was already expected to have a high barrier. Otherwise, the EDA reactant would dimerize spontaneously in the flask, and this is known experimentally not to be the case.

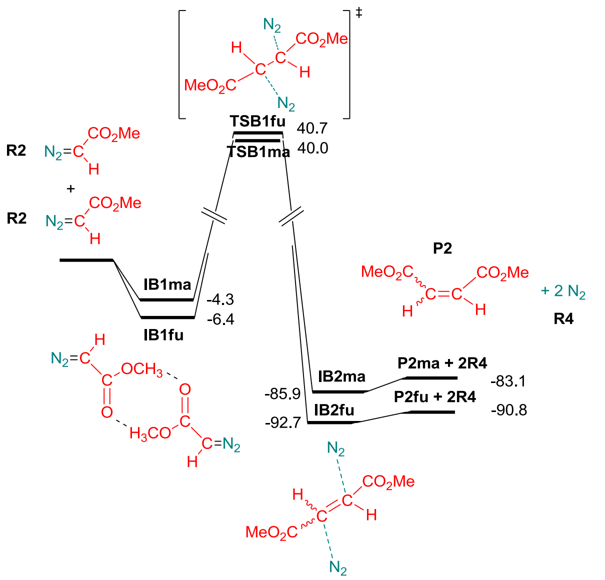

Figure 3: Energy profile (in kcal/mol) of the reaction between two N_2=C(H)(CO_3CH_3) giving fumarate and maleate compounds.

PathC

Figure 4 shows the general mechanism calculated for the production of fumarate and maleate species by reaction between N_2=C(H)(CO_2CH_3) and Tp^{Br3}M=C(H)(CO_2CH_3) (M = Ag, Cu). The relative potential energies of the corresponding stationary points for the different cases considered are collected in Table 2. The relative energies are much more moderate than in the case of **pathB** discussed above, and because of this, we will analyze this **pathC** in more detail. The sequence of steps for the coupling between N_2=C(H)(CO_2CH_3) and the corresponding metallocarbene complex takes place analogously to the mechanisms discussed before. The reactants approach to each other to afford an intermediate that evolves through a concerted transition state to form a carbon-carbon bond between the carbenic fragments of N_2=C(H)(CO_2CH_3) and Tp^{Br3}M=C(H)(CO_2CH_3).

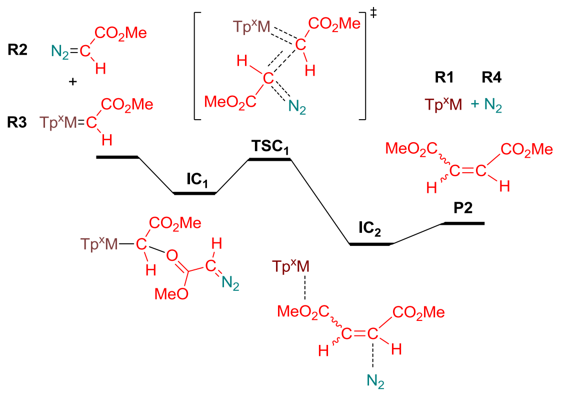

Figure 4: General pattern of the reaction between Tp^{Br3}M=C(H)(CO_2CH_3) and N_2=C(H)(CO_2CH_3) giving fumarate/maleate.

A significant quantitative difference with the other cases appears however in the relative energies of these **IC1**intermediates. The carboxylic oxygen of the diazo compound binds strongly the electrophilic carbenic carbon of the metallocarbene complex, resulting in the structures shown in Figure 5. The calculated energies presented in Table 2 show that such intermediates present a high stabilization with respect to the separated reactants, ca. 17 kcal/mol for the copper complexes,

Table 2. Potential energy (in kcal/mol) for the reaction between Tp^{Br3}M=C(H)(CO_2CH_3)(M=Ag,Cu) and N_2=C(H)(CO_2CH_3) giving fumarate (fu) and maleate (ma) derivatives.

M	prod.	IC1	TSC1	IC2	R1 + R4 + P2
Ag	ma	-28.9	-4.9	-109.4	-92.3
	fu	-29.4	-4.9	-114.6	-100.1
Cu	ma	-17.2	-4.1	-100.2	-80.9
	fu	-17.7	-4.0	-100.4	-88.8

and ca. 29 kcal/mol for the silver complexes. The high stability of this silver compound explains the experimental observation that the reaction gets blocked upon addition of high excesses of EDA to the reaction media. When a large excess of diazocompound is available at the reaction medium, the formation of this adduct may in practice reduce so much the concentration of the

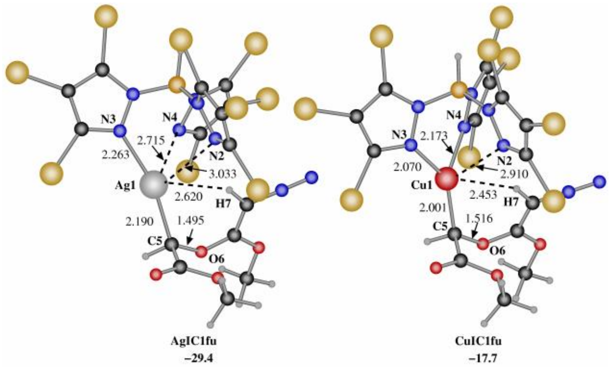

Figure 5: Optimized Becke3LYP structures of the intermediates **AgIC1fu** and **CuIC1fu** along the reaction path for the reaction between $Tp^{Br3}M=C(H)(CO_2CH_3)$ (M = Ag, Cu) and $N_2=C(H)(CO_2CH_3)$. Energies given in kcal/mol and distances in Å.

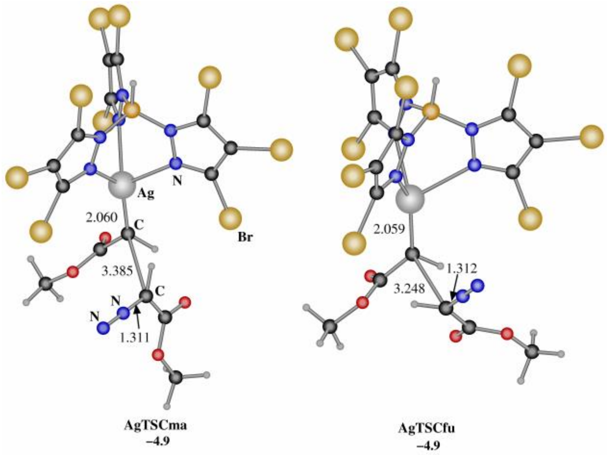

Figure 6: Optimized Becke3LYP structures of the transition states **AgTSC1ma** and **AgTSC1fu** along the reaction path for the reaction between $Tp^{Br3}Ag=C(H)(CO_2CH_3)$ and $N_2=C(H)(CO_2CH_3)$. Energies given in kcal/mol and distances in Å.

metallocarbene catalyst that the reaction is suppressed. On the other hand, this behaviour is not observed for the copper-based catalyst due to the lower stability of the adduct.

The difference in stability between the two adducts can be explained by the lower retrodonation between silver and carbon in the Ag-$C_{carbene}$ bond, that leaves the carbenic center more exposed to the electrophilic attack by the diazo compound. Figure 5 contains the optimized geometries for the intermediates **AgIC1fu** and **CuIC1fu**. In the former the distances Ag-$C_{carbene}$ and O-$C_{carbene}$ were calculated as 2.190 and 1.495 Å, respectively. When copper as the metal center, the corresponding metal-carbene distance is shorter (2.001 Å), while the bond distance O-$C_{carbene}$ is longer (1.516 Å).

The reaction continues through transition state **TSC1**. Figure 6 depicts the optimized geometries for the transition states when M = Ag. The relative potential energies for the transition states leading to fumarate and maleate product are the same, 4.9 kcal/mol below the separated reactants. This similarity agrees with the experimental observation of a mixture of both side-products. It is interesting to note that the breaking bond Ag-$C_{carbene}$ is very similar in both transition states, being 2.060 for **AgTSC1ma** and 2.059 Å for **AgTSC1fu**. The difference observed for the forming $C_{carbene}$-C_{diazo} bond distances is larger, being of 3.385 Å in the case of **AgTSC1ma** and 3.248 Å for **AgTSC1fu**. The results for the copper species are similar; the structures being contained in the Supporting Information.

After the transition state, the intermediate **IC2** is reached. At this point the product is already formed, though $Tp^{Br3}M$ (M = Cug, Ag) fragments remain bounded to the fumarate/maleate derivatives. **IC2** is far (more than 100 kcal/mol) below the separated reactants. Again, the profiles leading to fumarate and maleate are similar, confirming the mixture of both in the final outcome. It is worth mentioning that the highest energy point in the reaction profile is clearly transition state **TSC1**.

Competing pathways

From the results discussed within the different paths, it is obvious that only **pathA** and **pathC** can be proposed in temrs of their similar and low energy barriers. **PathA** provides the reaction main product, the functionalized alkane, whereas **pathC** leads to the side-products, fumarate/maleate. The results are in agreement in this sense with the experimental observations, and indicate that the side-products result from the reaction between the metallocarbene formed *in situ* and an additional EDA molecule.

Table 3. Free energies (in kcal/mol) for the highest energy points (TSA1, TSC1) in the competing paths leading to C-H insertion and sideproduct formation for each of the considered complexes.

	$Tp^{Br3}Ag$	$Tp^{Br3}Cu$
Insertion in CH_3CH_3	11.2	17.2
Insertion in $(CH_3)_2CH_2$	10.8	15.7
Maleate formation	6.9	9.1
Fumarate formation	6.9	8.0

A problem appears however when trying to translate the computational results into product ratios. For this, we should look into the highest energy point of each of the two pathways. We have converted the potential energy values reported above in free energies, but the trends are exactly the same. The values are collected in Table 3, where we focus in the activation of primary and secondary carbon-hydrogen bonds. We have neglected methane and tertiary carbon for simplicity: methane has necessarily a low concentration from a experimental point of view and, on the other hand, the fact that there is no barrier for C-H insertion in tertiary C-H bonds leads to a minor methodological problem). The results in Table 3 show that the free energies of the **TS** for C-H insertion oscillate between 10.8 and 17.2 kcal/mol, and those for fumarate/maleate formation are in the range between 6.9 and 9.1 kcal/mol. The direct comparison of the energy of these transition states would lead to the prediction that only the side-product should be formed, and that C-H insertion is minor at most.

However, one must take into account that the reaction rate does not depend only on energy barriers, but also on reactant concentrations. This is simply shown in equations (5) to (8), where the rate of consumption of the metallocarbene **MC** to produce either set of products is shown as a function of rate constants and reactant concentrations. The subscripts *A* and *C* stand for Activation and Coupling, respectively indicating the C-H functionalization or the formal carbene coupling.

$$-\frac{d[MC]}{dt} = v_A - v_B \tag{5}$$

$$v_A = k_A[MC][R-H] \tag{6}$$

$$v_C = k_C[MC][diazo] \tag{7}$$

$$\frac{v_A}{v_C} = \frac{k_A}{k_C}\frac{[R-H]}{[diazo]} \tag{8}$$

Transition state theory allows the connection of rate constants to energy barriers, and the expression can be further simplified by assuming identical pre-exponential factors A:

$$v_A = Ae^{-\Delta G_A^{\ddagger}/RT} \tag{9}$$

$$v_C = Ae^{-\Delta G_C^{\ddagger}/RT} \tag{10}$$

$$\frac{v_A}{v_C} = \frac{[R-H]}{[diazo]}e^{-\frac{(\Delta G_A^{\ddagger}-\Delta G_C^{\ddagger})}{RT}} \tag{11}$$

Equation (11) shows how the relative rate formation of the two products depends on the relative energies of the highest energy points, measured as $\Delta G^{\ddagger}_A$, $\Delta G^{\ddagger}_C$, and the concentrations in the reaction medium of the alkane substrate [R-H] and ethyl diazoacetate [diazo]. The relative energies play the expected critical role, with an exponential dependence on them. But the concentration effect is particularly important in this case, because the alkane is the solvent (thus in high concentration), and the diazocompound is a reactant that may be present in a very low concentration.

In fact, the concentration of the diazocompound is the only parameter that can be easily modified in the experimental conditions, and because of this we have isolated it in equation (12).

$$[diazo] = \frac{v_C}{v_A}[R-H]e^{-\frac{(\Delta G_A^{\ddagger}-\Delta G_C^{\ddagger})}{RT}} \tag{12}$$

Equation (12) presents the maximum concentration of the diazo reactant that would yield a given byproduct/product (ν_C/ν_A) ratio. If the concentration of diazocompound in solution is higher, the sideproduct will be more abundant than the desired ratio, if the concentration of diazocompound is lower, the insertion product will be more abundant. A last detail that has to be solved before the application of equation (12) is the assignment of a value to the alkane concentration [R-H]. This will depend on each particular alkane, but for the sake of an homogeneous comparison, we have settled on the concentration of 7.64 mol/l for commercially available 2,3-dimethylbutane, which is often used in this type of reactions.

Table 4 shows the values obtained by application of Eq. 11. Two scenarios are considered: i) a highly efficient process, where only 1% of maleate and fumarate is formed; ii) a medium efficiency process, where half of the reactant is converted into fumarate/maleate sideproducts. It is clear in the Table 4 that the silver complex tolerates much higher values of free diazocompound in solution. For instance, insertion into secondary

Table 4. Maximum diazo-compound concentration to obtain 1 or 50% of by-product by application of the Eq.12.

	[diazo] for 1% of by-product		[diazo] for 50% of by-product	
R	**[$Tp^{Br3}Ag$]**	**[$Tp^{Br3}Cu$]**	**[$Tp^{Br3}Ag$]**	**[$Tp^{Br3}Cu$]**
CH_3CH_3	$5.4.10^{-5}$	$1.4.10^{-8}$	$5.4.10^{-3}$	$1.4.10^{-6}$
$(CH_3)_2CH_2$	$1.1.10^{-4}$	$1.8.10^{-7}$	$1.1.10^{-2}$	$1.7.10^{-5}$

C-H will be already the main reaction (above 50%) with diazo concentrations below $1.1.10^{-2}$ M. This can be achieved with copper compounds only if the concentration is below $1.7.10^{-5}$ M. This result perfectly fits with the experimental observation that the reaction must proceed through careful slow addition of EDA only in the case of the copper complex. The slow addition allows the consumption of practically all diazocompound in formation of the reacting carbene complex, with nearly no diazocompound left free in solution. The concentration of the diazocompound is not so critical in the case of silver, which therefore does not require special caution in the EDA addition.

The importance of concentration effects also explains the special difficulty of methane activation with this type of catalysts. Methane is not liquid at room temperature, it cannot be used as solvent in these conditions, and it cannot benefit from the heavy concentration effect in favour of more conventional alkanes.

Conclusion

DFT calculations have allowed the clarification of the mechanism for the undesired generation of fumarate and maleate derivatives in the metal-catalyzed carbene insertion into the C-H bonds of alkanes. The transient metallocarbene $Tp^{Br3}M{=}C(H)(CO_2CH_3)$ (M = Cu, Ag) is acting as key reacting species in both the main and the side reactions. In the main reaction the metallocarbene reacts with an alkane molecule and functionalizes the C-H bond, while in the side reaction, it reacts with a diazo compound molecule to produce either fumarate of maleate.

The nature of the metal center plays an important role in the relative rates of the reactions. The generation of fumarate/maleate species is more favourable with copper than with silver complexes, in good agreement with the experimental observation that special care must be taken when using copper complexes. The presence of a stable adduct between the silver metallocarbene species and the diazo compound also explains the experimentally observed blocking of the reaction by high excesses of the latter.

A better understanding of the competing reactions is a first step towards the development of more efficient processes, and this could only be achieved with the application of computational methods to a better understanding of the role of the reactivity of transient species as $Tp^{Br3}M{=}C(H)(CO_2CH_3)$.

Computational Section

Calculations were performed at the DFT level, by means of Becke3LYP[12-14] functional, with a hybrid Becke3 exchange functional and a Lee-Yang-Parr correlation functional [12,13], using the Gaussian suite of programs [15]. Cu, Ag and Br atoms were described using an effective core potential (LANL2DZ) for the inner electrons [15,16], and its associated double-ζ basis set for the outer ones. An additional f polarization shell was added for Cu and Ag, with exponents of 3.525 and 1.611 respectively [17]. In the case of Br, a d polarization shell was added (exponent 0.4280).[18] The 6-31G(d) basis set was used for the H, B, C, N and O atoms.[19] The structures of the reactants, intermediates, transition states and products were fully optimized without any symmetry restriction. Transition states were identified by having one imaginary frequency in the Hessian matrix. Free energy corrections at 298 K and 1 atm pressure were added in selected cases following the standard statistical mechanics procedures.

Acknowledgements

Financial support from the ICIQ foundation, the Spanish MEC (projects CTQ2008-06866-CO2-02/BQU, CTQ2008-00042/BQU, Consolider Ingenio 2010 CSD2006-0003) and the Catalan DURSI (project 2009SGR0259) is acknowledged.

Keywords: C-H functionalization • homoscorpionate • diazo compound metallocarbene • coinage metal • DFT

[1] a) R. H. Crabtree, *Chem. Rev.* **2010**, *110*, 575; b) R. G. Bergman, *Nature* **2007**, *446*, 391; c) J. A. Labinger, J. E. Bercaw, *Nature* **2002**, *417*, 507; d) K. I. Goldberg, A. S. Goldman (Eds) *Activation and Functionalization of C-H Bonds* (ACS Symp. Ser. 885, Am. Chem. Soc., Washington DC, **2004**).

[2] a) A. E. Shilov, G. B. Shul'pin in *Activation and Catalytic Reactions of saturated hydrocarbons in the presence of metal complexes*, Kluwer, Dordrecht , **2000**; b) G. Dyker, *Angew. Chem., Int. Ed. Engl.* **1999**, *28*, 1698; c) Y Guari, S. Sabo-Etienne, B. Chaudret, *Eur. J. Inorg. Chem.* **1999**, 1047; d) A. E. Shilov, G. B. Shul'pin, *Chem Rev.* **1997**, *97*, 2879; f) B. A. Arndtsen, R. G. Bergman, T. A. Mobley, T. H. Peterson, *Acc. Chem Res.* **1995**, *28*, 154.

[3] a) M. P. Doyle, R. Duffy, M. Ratnikov, L. Zhou, *Chem. Rev.* **2010**, *110*, 704; b) M. P. Doyle, M. A. McKervey, T. Ye, *Modern Catalytic Methods for Organic Synthesis with Diazo Compounds*; John Wiley & Sons: New York, **1998;** c) H. M. L. Davies, T. Hansen, M. R. J. Churchill, *J. Am. Chem. Soc.* **2000**, *122*, 3063; d) H.-Y. Thu; G. S.-M. Tong, J.-S. Huang, S. L.-F. Chan, Q.-H. Deng, Che, C.-M. *Angew. Chem. Int. Ed.* **2008,** *47*, 9747.

[4] M. M. Díaz-Requejo, T. R. Belderrain, M. C. Nicasio, P. J. Pérez, *Dalton Trans.* **2006**, 5559; M. M. Díaz-Requejo, P. J. Pérez, *Chem. Rev.* **2008**, *108*, 3379.

[5] a) M. M. Díaz-Requejo, T. R. Belderrain, M. C. Nicasio, S. Trofimenko, P. J. Pérez, *J. Am. Chem. Soc.* **2002**, *124*, 896. b) A. Caballero, M. M. Díaz-Requejo, T. R. Belderrain, M. C. Nicasio, S. Trofimenko, P. J Pérez, *J. Am. Chem. Soc.* **2003**, *125*, 1446. c) A. Caballero, M. M. Díaz-Requejo, T. R. Belderrain, M. C. Nicasio, S. Trofimenko and P. J Pérez, *Organometallics* 2003, **22**, 4145. d) E. Despagnet-Ayoub, K. Jacob, L. Vendier, M. Etienne, E. Álvarez, A. Caballero, M. M. Díaz-Requejo, P. J. Pérez, *Organometallics* **2008**, *27*, 4779.

[6] a) J. Urbano, T. R. Belderraín, M. C. Nicasio, S. Trofimenko, M. M. Díaz-Requejo, P. J. Pérez, *Organometallics* **2005**, *24*, 1528. b) H. V. R. Dias, R. G. Browning, S. A. Richey, C. J. Lovely, *Organometallics* **2005**, *24*, 5784. c) H. V. R. Dias, R. G. Browning, S. A. Richey, C. J. Lovely, *Organometallics* 2004, **23**, 1200.

[7] For copper-based metallocarbene intermediates detected see: (a) B. F. Straub, P. Hofmann, *Angew. Chem., Int. Ed. Engl*. **2001**, *40*, 1288. (b) X. L. Dai, T. H. Warren, *J. Am. Chem. Soc*., **2004**, *126*, 10085.

[8] E. Nakamura, N. Yoshikai, M. Yamanaka, *J. Am. Chem. Soc.* **2002**, *124*, 7181.

[9] A. A. C. Braga, F. Maseras, J. Urbano, A. Caballero, M. M. Díaz-Requejo, P. J. Pérez, *Organometallics* **2006**, *25*, 5292.

[10] J. Urbano, A. A. C. Braga, F. Maseras, E. Álvarez, M. M. Díaz-Requejo, P. J. Pérez, *Organometallics* **2009**, *28*, 5968.

[11] A. Caballero, M. M. Díaz-Requejo, S. Trofimenko, T. R. Belderrain, P. J. Pérez, *Eur. J. Inorg. Chem.* **2007**, 2848.

[12] C. Lee, R. G. Parr, W. Yang, *Phys. Rev. B* **1988**, 37, 785.

[13] A. D. Becke, *J. Chem. Phys.* **1993**, 98, 5648.

[14] P. J. Stephens, F. J. Devlin, C. F. Chabalowski, M. J. Frisch, *J. Phys. Chem.* **1994**, 98, 11623.

[15] M. J. Frisch, et al. *Gaussian 03, Revision C.02*, Gaussian, Inc., Wallingford, CT, **2004**.

[16] W. R. Wadt, P. J. Hay, *J. Chem. Phys.* **1985**, 82, 284.

[17] A. W. Ehlers, M. Böhme, S. Dapprich, A. Gobbi, A. Höllwarth, V. Jonas, K. F. Köhler, R. Stegmann, A. Veldkamp, G. Frenking, *Chem. Phys. Lett.* **1993**, 208, 111.

[18] A. Höllwarth, M. Böhme, S. Dapprich, A. W. Ehlers, A. Gobbi, V. Jonas, K. F. Köhler, R. Stegmann, A. Veldkamp, G. Frenking, *Chem. Phys. Lett.* **1993**, 208, 237.

[19] M. M. Francl, W. J. Pietro, W. J. Hehre, J. S. Binkley, M. S. Gordon, D. J. Defrees, J. A. Pople, *J. Chem. Phys.* **1982**, *77*, 3654.

Received: ((will be filled in by the editorial staff))
Published online: ((will be filled in by the editorial staff))

DFT studies have shown that the generation of fumarate/maleate dimers as non-desired products during the catalytic functionalization of alkanes by carbene insertion from diazocompounds occurs through a metallocarbene-diazocompound interaction. The calculations have allowed to predict the exact catalyst-to-diazocompound ratio that minimizes the formation of such those sideproducts.

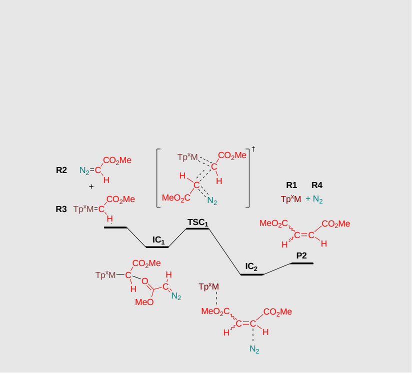

Ataualpa A. C. Braga,[a] Ana Caballero,[b] Juan Urbano,[b] M. Mar Diaz-Requejo,[b] Pedro J. Pérez*[b] and Feliu Maseras*[a].

The Mechanism of By-side Reactions in Alkane C-H Bond Functionalization by Coinage Homoscorpionate Complexes: A DFT study